Raman-spectroscopic investigations on the crystal structure and phonon modes of Ba(RE$_{1/2}$Ta$_{1/2}$)O$_3$ microwave ceramics

Roberto L. Moreira [a,*], L. Abdul Khalam [b], Mailadil T. Sebastian [b], Anderson Dias [c]

[a] *Departamento de Física, ICEx, UFMG, C.P. 702, Belo Horizonte 30123-970, MG, Brazil*
[b] *Ceramic Technology Division, Regional Research Laboratory, Trivandrum 695019, India*
[c] *Departamento de Química, ICEB, UFOP, Ouro Preto 35400-000, MG, Brazil*

Available online 14 December 2006

Abstract

Complex Ba(RE$_{1/2}$Ta$_{1/2}$)O$_3$ [RE = rare earth] ceramics have been prepared by solid state ceramic route and their microwave dielectric responses were measured in the GHz range. In general, the resonators showed high dielectric constants, high quality factors and good thermal stability of the resonance frequency. However, these properties are found to depend nonlinearly on the tolerance factor, indicating structural modifications with chemical substitution. The structure of Ba(RE$_{1/2}$B$''_{1/2}$)O$_3$ [B$''$ = Nb, Ta] compounds has been a matter of debate for many years, because X-ray structural data and vibrational-spectroscopic ones are controversial. In order to contribute to this debate and discuss the relationship between structure and dielectric properties, a systematic investigation of the phonon modes of several ceramics with varying RE ion was carried out. In this paper, the results of the Raman analysis and crystal structure of Ba(RE$_{1/2}$Ta$_{1/2}$)O$_3$ samples are presented, and correlated with the observed microwave dielectric properties.
© 2006 Elsevier Ltd. All rights reserved.

Keywords: Sintering; Spectroscopy; Dielectric properties; Perovskites; Capacitors

1. Introduction

Ceramic materials with ABO$_3$ perovskite structure are being currently used in a large number of technological applications, such as transducers, sensors, capacitors (polar materials), dielectric resonators and filters (centrosymmetric compounds).[1] These materials offer the possibility of tailoring and optimising the required dielectric properties, because of the many possibilities of cation substitution or mixing in the A or B sites. In particular, the rapid development of microwave-based wireless telecommunications is favouring the search for new materials with adequate structure (i.e., centrosymmetric) and good dielectric response, which means low-loss ceramics with high and thermally stable dielectric constant.[2] Among the important dielectric resonators studied so far, a large number of works have been devoted to Ba$_2$Ti$_9$O$_{20}$,[3] Zr(Sn,Ti)O$_4$,[4] Ba$_5$Nb$_4$O$_{15}$,[5] and to complex perovskites of general formula A(B$'_{1/3}$B$''_{2/3}$)O$_3$.[6–8] On the other hand, A(B$'_{0.5}$B$''_{0.5}$)O$_3$ materials have received much less attention,[9–11] although it has been recently showed that

Ba(RE$_{0.5}$B$''_{0.5}$)O$_3$ ceramics, where RE is a rare-earth ion and B$''$ = Nb or Ta, present quite adequate microwave dielectric responses.[12–14]

The microwave properties of Ba(RE$_{1/2}$B$''_{1/2}$)O$_3$ [B$''$ = Nb, Ta] compounds are found to depend nonlinearly on the RE ionic radii, because of possible structural modifications with chemical substitution. However, the structure of these materials has been a matter of debate for many years, because X-ray structural data and vibrational-spectroscopic ones obtained by different authors are controversial.[10,15–21] In a recent work, we have investigated the Raman phonon modes of several Ba(RE$_{1/2}$Nb$_{1/2}$)O$_3$ compounds, showing that tetragonal and orthorhombic structures were compatible with the observed features, with the phase transformation occurring with increasing ionic radius.[22] In this work, the evolution of the dielectric response and the structural changes of Ba(RE$_{1/2}$Ta$_{1/2}$)O$_3$ compounds are studied.

The structure of Ba(Y$_{1/2}$Ta$_{1/2}$)O$_3$ compound was shown to be cubic belonging to the $Fm\bar{3}m$ ($Z = 4$)[10,17–19,21] with a low-temperature phase transition (PT) to a tetragonal ($I4/m$, $Z = 4$) structure around $-20\,°C$.[17–19] The same PT sequence with temperature was observed at high temperatures for Gd and Nd compounds, so that these materials would have the tetragonal structure at room temperature,[18,19] confirming the proposition of

Galasso et al.[10,15] for Gd. On the other hand, Doi and Hinatsu[21] claimed recently that $Ba(RE_{1/2}Ta_{1/2})O_3$ would present cubic, for Y and RE = Lu–Dy, or monoclinic $P2_1/n$ ($Z = 4$) structures, for RE = Tb–La, in disagreement with the tetragonal structures above for Gd and Nd. Also, although the materials with cubic structures of Doi and Hinatsu[21] agree with those of Galasso et al.,[10,15] the latest authors proposed an orthorhombic *Pbnm* ($Z = 4$) structure for the compound with lanthanum. In view of that, the goal of this work is to present the results on the optical phonon modes and microwave dielectric behaviour of $Ba(RE_{1/2}Ta_{1/2})O_3$ ceramics (RE = Y, La, Nd–Ho, and Yb). Detailed X-ray diffraction around chosen Bragg reflections was also used together with spectroscopic data in order to infer the most probable symmetries for these materials.

2. Experimental

$Ba(RE_{1/2}Ta_{1/2})O_3$ [RE = La, Nd, Sm, Eu, Gd, Tb, Dy, Ho, Y, and Yb] ceramics were prepared by the conventional solid state ceramic route. High purity $BaCO_3$ (99.9%, Aldrich Chemicals, Milwaukee WI, USA), Ta_2O_5 (99.9%, Nuclear Fuel Complex, Hyderabad, India), and rare-earth oxides (99.9%, Indian Rare Earths Ltd., Udyogamandal, India) were weighed in the stoichiometric ratio 4:1:1 and ball milled using zirconium balls in distilled water medium for 5 days. The slurries were dried and calcined at 1375 °C for 4 h. The calcined materials were ground, mixed thoroughly with 3 wt.% PVA solution and dried. They were again ground and uniaxially pressed into cylindrical compacts of 11–14 mm diameter and height 6–7 mm under a pressure of 100–125 MPa. The obtained compounds were sintered in air at 1625 °C, for 4 h. Nb_2O_5 (0.5 wt.%) was added to the calcined powder of the compounds with RE = La, Eu, Gd, Tb, and Y, as sintering aid, aiming to obtain maximum densification (up to 97–99% of the theoretical densities). For the Dy sample, 0.5 wt.% of CeO_2 was used, while for RE = Ho and Yb a mixture of 0.5 wt.% of Nb_2O_5 and CeO_2 showed the best results. The bulk densities of the sintered samples were measured by Archimedes method. Well-polished samples were used for all the measurements.

The microwave dielectric properties were measured in the region 4–6 GHz using a 8753 ET Network Analyser. The dielectric constants were obtained by using the TE_{011} mode from the method of Hakki and Coleman,[23] while the quality factors were calculated from $TE_{01\delta}$ mode by the cavity method.[24] The temperature coefficient of the resonance frequency (τ_f) was measured for each sample by considering the temperature variation of the $TE_{01\delta}$ resonance mode in the temperature range 25–70 °C. X-ray diffraction was performed in a modified Rigaku powder apparatus (Geigerflex 2037), equipped with a Cu Kα source (40 kV, 30 mA) and graphite monochromator, from 10° to 100° 2θ, with 15 s accumulations for each 0.02° 2θ step. The Raman spectra of the samples were collected in back-scattering configuration with an Olympus microscopy (100× objective) attached to a Dilor XY spectrometer. The 514.5 nm line of an Ar$^+$ laser (12 mW) was used as exciting line, and detection was carried out by a liquid-nitrogen cooled CCD. The spectral resolution was better than 2 cm^{-1} and the accumulation times were typically

three collections of 60 s. The obtained spectra were divided out by the Bose factor[25] before being fitted by a sum of Lorentzian lines.

3. Results and discussion

The microwave dielectric responses of the $Ba(RE_{1/2}Ta_{1/2})O_3$ ceramic samples were measured in the range 4–6 GHz and the results are presented in Table 1, together with the measured densities (% of the theoretical values) and the tolerance factors (t), calculated according to the proposition of Reaney et al.[26] Once Nb^{5+} and Ta^{5+} have the same ionic radii, the t values are the same as in the $Ba(RE_{1/2}Nb_{1/2})O_3$ compounds.[13] Table 1 shows that the use of sintering aids led to very dense samples with relatively uniform dielectric constants (continuous increasing of ε_r from Yb to Nd, then a small decrease for La). However, the unloaded quality factors ($Q_u \times f$) vary significantly, probably originated from extrinsic losses due to microstructural features (grain sizes and boundaries, space charges) rather than from the intrinsic polar phonons, once infrared measurements in these samples showed quite similar spectra (these spectra are not shown here).

The results showed in Table 1 evidence a close relationship between structure and properties for the $Ba(RE_{1/2}Ta_{1/2})O_3$ ceramics. Particularly, the temperature coefficients of the resonant frequency, τ_f, change drastically as a function of the tolerance factors, as it is shown in Fig. 1. The vertical dashed lines in this figure indicate approximately critical t values, according to Reaney et al.[26] It was observed that τ_f varies from high positive values (for Yb, Ho and Y samples) to small negative ones for the other samples. High positive τ_f (together with t close to 1) is characteristic of cubic structures, while negative values for $t < 0.985$ are indications of structures of lower symmetries, usually showing distorted or tilted octahedra.[26] Therefore, these simple results from macroscopic dielectric response and tolerance factors give us a first indication of lowering symmetry for our samples, though its important to remember that the indicated lines for tilting changes are temperature dependent and may vary for particular samples.[22,26]

In order to verify the possible lowering of symmetry from Ho to Dy sample and others, we have initially performed X-ray powder diffraction around some strong Bragg reflections. We used the indices for the cubic $Fm\bar{3}m$ phase, since this phase

Table 1
Measured densities (ρ) and microwave dielectric response (ε_r, Q_u at 4–6 GHz, and τ_f) for the $Ba(RE_{1/2}Ta_{1/2})O_3$ ceramic samples together with the tolerance factors (t)

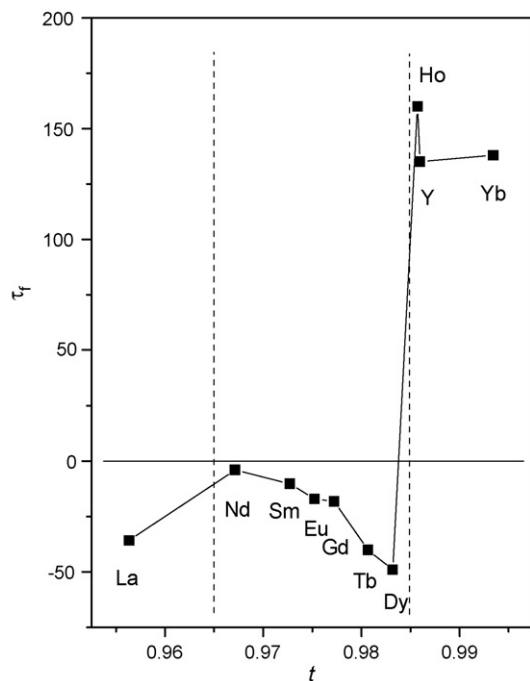| RE	ρ (%)	t	ε_r	$Q_u \times f$ (GHz)	τ_f (ppm/°C)
La	97.5	0.95633	37.1	20950	−35.7
Nd	98.0	0.96712	38.7	12050	−4.00
Sm	96.0	0.97272	37.6	15000	−10.2
Eu	97.0	0.97521	36.5	41200	−16.2
Gd	97.0	0.97725	36.0	3150	−18.2
Tb	98.0	0.98067	35.5	31900	−38.2
Dy	97.5	0.98320	34.0	20650	−48.0
Ho	98.0	0.98573	33.5	24050	130.0
Y	96.0	0.98597	33.0	50150	120.0
Yb	98.0	0.99343	32.0	35850	112.0

Fig. 1. Temperature coefficient of the resonant frequency (τ_f) as a function of the tolerance factor t for Ba(RE$_{1/2}$Ta$_{1/2}$)O$_3$ ceramics. The vertical dashed lines indicate approximately the critical values of t according to Reaney et al.[26]

has been currently accepted for Y sample. The peaks chosen were (4 0 0), (4 4 0) and (6 2 0), located approximately at 42°, 62° and 70° 2θ, respectively. Fig. 2a presents the diffractograms for the Ba(RE$_{1/2}$Ta$_{1/2}$)O$_3$ ceramics in the range 67–72° 2θ, i.e., a detail for the cubic (6 2 0) peak. The doubling of the reflections for Yb, Y and Ho accounts for the K$_{\alpha 1}$ (1.54051 Å) and K$_{\alpha 2}$ (1.54433 Å) lines. For the sample with Dy, a small peak broadening and a faint shoulder at lower angles indicate the appearing of ferroelastic domains, accompanying the phase transformation cubic-to-tetragonal. For the Tb sample, a third peak appears clearly and the ferroelastic distortion shows to be more important, becoming still larger for Gd and Eu. For the latest three samples, although the existence of ferroelastic domains is also clear, the peak profiles are quite different, they look like if the number of domains has increased. A second ferroelastic transition from tetragonal to orthorhombic or monoclinic structure would lead to such behaviour. The same features were observed for the (4 4 0) cubic peak (Fig. 2b), while the (4 0 0) reflection showed only a broadening for samples from Dy to La, without revealing details about ferroelastic domains (Fig. 2c).

The results of the X-ray diffraction confirmed the predicted phase transformation between Ho and Dy samples, conjectured from the observed behaviour of τ_f versus t (Table 1 and Fig. 1), and also the ferroelastic nature of such transformation. Besides, they suggested a second transition to a still lower symmetry phase for samples with RE = Sm, Nd and La. Raman spectroscopy is a very powerful tool to investigate the symmetries of crystalline structures, due to the very strict selection rules. For our system, at our knowledge, only Ba(Y$_{1/2}$Ta$_{1/2}$)O$_3$ sample has been previously investigated by Raman spectroscopy.[19] Therefore, we have undertaken Raman measurements of all samples.

The obtained spectra are presented in Fig. 3 (RE = Yb, Y and Ho), Fig. 4 (RE = Dy, Tb, Gd and Eu), and Fig. 5 (RE = Sm, Nd and La). In general, the ceramics present a highly ordered structure because the Raman lines are of narrow width. It is also clear that three types of Raman spectra are observed, accordingly to the displayed figures (the samples were grouped according to the number of observed features).

For the first group of samples (Yb, Y and Ho), the number of observed bands corresponds well to that predicted by group theory[27] for the cubic $Fm\bar{3}m$ (O_h^5) group. For this structure, the reducible representation at the Brillouin zone centre calculated with Ba ions at 8c Wyckoff sites of T_d symmetry, RE at 4a (O_h), Ta at 4b (O_h) and O at 24e (C_{4v}) sites is $\Gamma = A_{1g} + E_g + F_{1g} + 2F_{2g} + 5F_{1u} + F_{2u}$.[19,22] Therefore, four Raman-active bands (A$_{1g}$, E$_g$ and F$_{2g}$) are expected, which correspond to the observed features at 101 and 384 cm^{-1} (F$_{2g}$), 760 cm^{-1} (E$_g$) and 838 cm^{-1} (A$_{1g}$), for the Y compound. These assignments are in complete agreement with those of Ref.[19] for the same ceramic. The results of the fits for the ceramics with Yb and Ho are presented in Table 2, together with the band characteristics for Y. We should also notice a relatively high luminescence of the Ho compound (corrected here) and the presence of one extra weak Raman feature for all samples, located around 311 cm^{-1}. As it will be shown in the sequence, this band appears for all samples and is not characteristic of the cubic phase. Therefore, we believe that some locally induced lattice distortions of the cubic structure are present, originated from stresses generated during cooling or due to the presence of some extrinsic defects.

Let us now analyze the second group of samples, presented in Fig. 4. For these materials, nine bands are clearly seen at 104, 311, 382, 411, 527, 557, 704, 749 and 828 cm^{-1} (for the Eu compound). The fitting parameters for the Dy, Tb, Gd and Eu samples are presented in Table 3. Now, we look for the reduced representation for these materials at the Brillouin Γ-point. For the tetragonal $I4/m$ (C_{4h}^5) structure, the site positions (and symmetries) for the atoms are[10,15]: Ba in 4d (S$_4$), RE in 2a (C_{4h}), Ta in 2b (C_{4h}), O1 in 8h (C_s) and O2 in 4e (C_4). Thus, by using the factor group method,[27] one has: $\Gamma = 3A_g + 3B_g + 3E_g + 5A_u + B_u + 6E_u$. The relationship between O_h and C_{4h} groups allows us to establish the correlation between modes of both structures.[27] Moreover, once the volume of the primitive cell is the same for both phases, all modes of the lower symmetry phase come from vibrations at the Brillouin Γ-point. However, the absence of useful symmetry rules for the different irreducible representations (due to the polycrystalline nature of the sample) makes difficult and prac-

Table 2
Raman fitting parameters for Ba(RE$_{1/2}$Ta$_{1/2}$)O$_3$ ceramics with cubic structure

Band	Yb	Y	Ho
1	109 (12)	101 (10)	103 (11)
2	392 (21)	384 (15)	390 (17)
3	769 (59)	760 (48)	764 (41)
4	841 (26)	838 (35)	841 (28)

Position and full width at half-maximum (in parentheses) are in cm^{-1}.
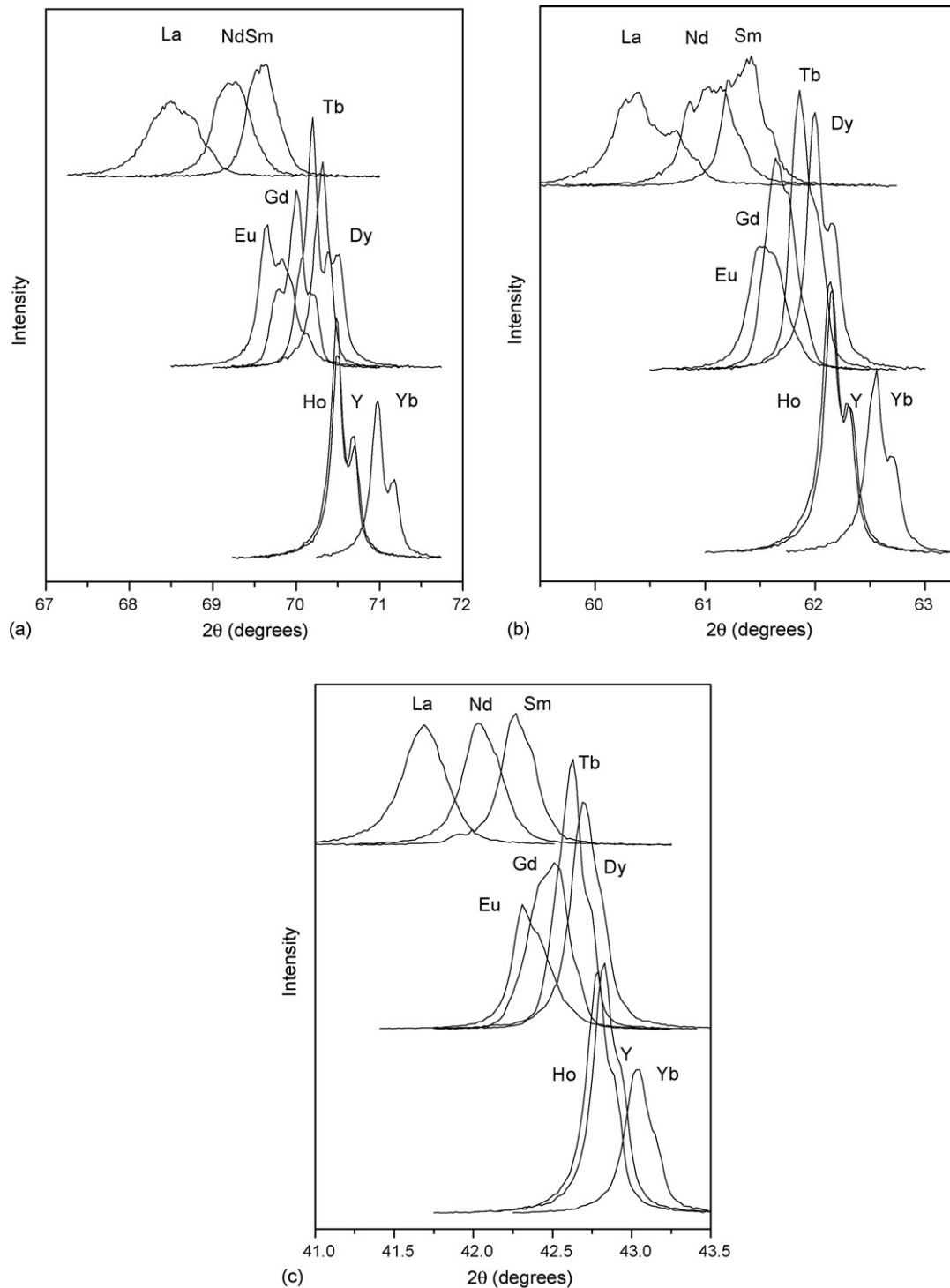
Fig. 2. X-ray powder diffraction for the Ba(RE$_{1/2}$Ta$_{1/2}$)O$_3$ ceramics. (a) Detail for the range 67–72° 2θ, showing the splitting of the cubic (6 2 0) peak. Doubling of the reflections for Yb, Y and Ho accounts for K$_{\alpha1}$ (1.54051 Å) and K$_{\alpha2}$ (1.54433 Å) lines. (b) Detail for the range 59.5–63.3° 2θ, around the cubic (4 4 0) peak. (c) Detail for the range 41.0–43.5° 2θ, around the cubic (4 0 0) peak.

tically useless a complete mode assignment for the observed bands. Anyway, it is clear the peak splitting of the cubic E$_g$ mode (leading to the band #7 of the tetragonal structure) and F$_{2g}$ bands (new band #4). Finally, it is important to remark the high coherence between the results from Raman spectra for the tetragonal phase with the observations of the splitting of Bragg peaks and the sign variations of τ_f.

The latest group of samples presented a number of Raman modes clearly higher than 9 (Fig. 5). In particular, we can see the peak splitting for the two cubic F$_{2g}$ modes around 105 and 380 cm^{-1}, which transform each one in three modes, respectively, numbers 1, 2, 3 and 8, 9, 10 in Table 4. This table presents the results of the fit of the spectra of Sm, Nd and La samples by a sum of Lorentzian lines. Only 16 bands are seen,
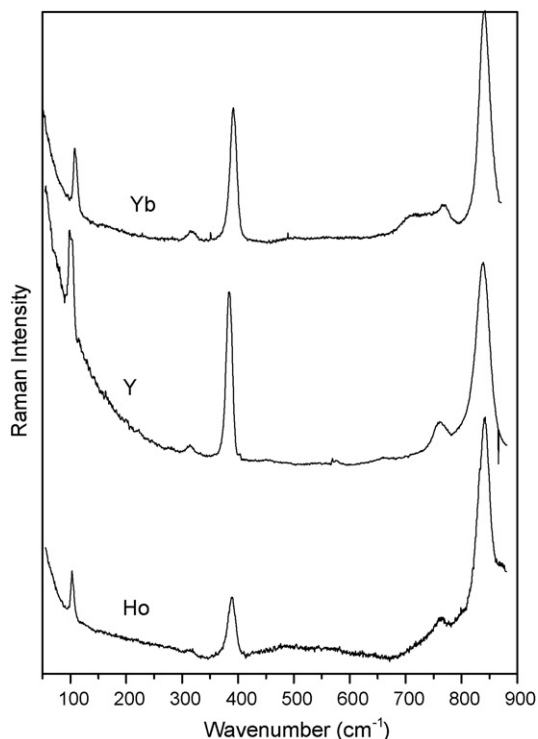
Fig. 3. Micro-Raman spectra of the Ba($RE_{1/2}Ta_{1/2}$)O$_3$ ceramics [RE = Yb, Y, and Ho] with cubic symmetry.

Fig. 5. Micro-Raman spectra of the Ba($RE_{1/2}Ta_{1/2}$)O$_3$ ceramics with RE = Sm, Nd and La (orthorhombic symmetry).

since we have avoided bands that are not clearly seen. Now, if we consider the two lower symmetry structures proposed for these materials, i.e., orthorhombic[15] and monoclinic[21] (we discard the tetragonal proposition for Nd of Refs.[18,19]), it is
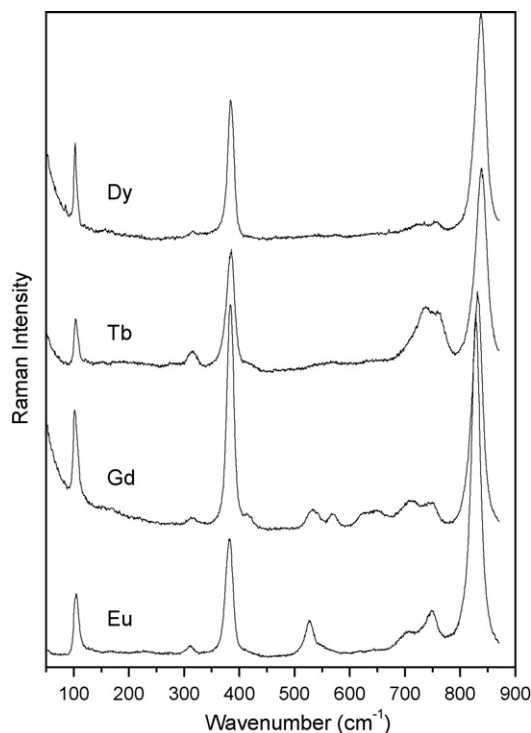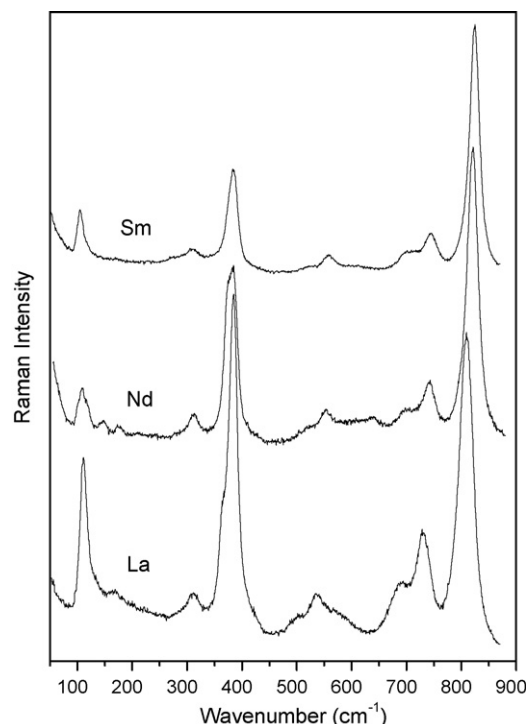

Fig. 4. Micro-Raman spectra for tetragonal Ba($RE_{1/2}Ta_{1/2}$)O$_3$ ceramics [RE = Dy, Tb, Gd and Eu].

possible to calculate the number of Raman predicted modes for each case. We found 24 non-degenerated Raman-active modes for both, orthorhombic *Pbnm* (D_{2h}^{16}) and monoclinic *P*2$_1$/*n* (C_{2h}^{5}) structures, with the following reducible representations at the Brillouin zone centre (Wyckoff sites taken from Refs.[15,21]): $\Gamma_{\text{ortho}} = 7A_g + 5B_{1g} + 7B_{2g} + 5B_{3g} + 8A_u + 10B_{1u} + 8B_{2u} + 10B_{3u}$ and $\Gamma_{\text{mono}} = 12A_g + 12B_g + 18A_u + 18B_u$ (all g = *gerade* modes are Raman active). If we were dealing with single crystalline samples, it would be quite simple to decide above the two groups above by using polarized Raman spectra, since the totally symmetric vibrations would be seen only in parallel polarizations and also cross-polarized spectra would be very different for different scattering symmetries. However, for our case, where unpolarized spectra of polycrystalline samples are obtained, it is not possible to take benefit of such symmetry rules.

Table 3
Raman fitting parameters for Ba($RE_{1/2}Ta_{1/2}$)O$_3$ ceramics with tetragonal symmetry

Band	Dy	Tb	Gd	Eu
1	103 (7)	104 (9)	102 (10)	104 (14)
2	318 (34)	316 (20)	315 (25)	311 (17)
3	386 (17)	385 (25)	384 (18)	382 (22)
4	416 (50)	415 (37)	413 (25)	411 (29)
5	548 (52)	545 (45)	533 (27)	527 (22)
6	572 (49)	571 (48)	569 (16)	557 (40)
7	720 (44)	725 (32)	711 (37)	704 (22)
8	758 (42)	759 (32)	751 (30)	749 (25)
9	837 (30)	834 (34)	832 (36)	828 (28)

Position and full width at half-maximum (in parentheses) are in cm^{-1}.

Table 4
Raman fitting parameters for Ba(RE$_{1/2}$Ta$_{1/2}$)O$_3$ ceramics with orthorhombic structure

Band	Sm	Nd	La
1	97 (5)	99 (6)	104 (8)
2	104 (10)	110 (11)	112 (16)
3	116 (7)	118 (11)	121 (13)
4	145 (22)	147 (13)	145 (25)
5	172 (28)	176 (15)	167 (20)
6	275 (45)	278 (40)	278 (35)
7	310 (21)	311 (22)	311 (19)
8	369 (14)	372 (12)	363 (13)
9	384 (20)	385 (24)	385 (22)
10	418 (39)	421 (38)	425 (31)
11	524 (34)	523 (27)	502 (31)
12	558 (25)	553 (22)	535 (42)
13	639 (38)	639 (20)	630 (40)
14	702 (35)	697 (36)	683 (38)
15	744 (22)	742 (19)	730 (21)
16	824 (32)	821 (34)	808 (40)

Position and full width at half-maximum (in parentheses) are in cm^{-1}.

Although the Raman spectra alone are not enough to allow us to conclude about the correct space group for samples with Sm, Nd and La, it is believed that the correct one would be *Pbnm*, similarly to Ba(RE$_{1/2}$Nb$_{1/2}$)O$_3$ compounds with the same lanthanides.[22] Indeed, as it was shown in that work, X-ray diffraction of these higher ionic radius lanthanides showed small reflections around 34°, 36° and 46° 2θ, which are compatible with the orthorhombic structure, but not with the monoclinic
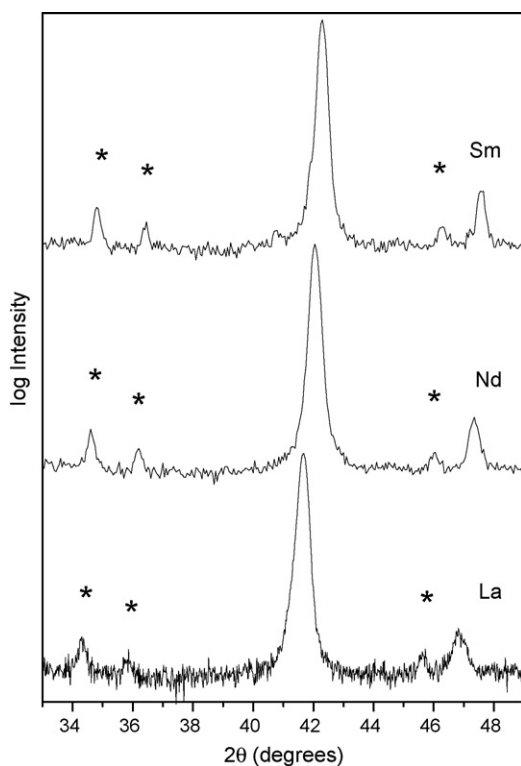

Fig. 6. X-ray diffractograms for the Ba(RE$_{1/2}$Ta$_{1/2}$)O$_3$ ceramics with RE = Sm, Nd and La, in the 33–49° 2θ range, in which peaks with asterisks are only compatible with an orthorhombic symmetry.

one. The presence of these peaks for Ba(RE$_{1/2}$Ta$_{1/2}$)O$_3$ compounds (RE = Sm, Nd and La) was also observed, as it is shown in Fig. 6.[22] Based on these results, it is reasonable to assume that an orthorhombic *Pbnm* structure accounts for the observed Raman modes in Sm, Nd and La ceramics. This is in perfect agreement with X-ray diffraction and microwave dielectric results for these materials.

As a general trend, for frequencies above 600 cm^{-1} a shift to lower frequencies was observed as a function of ionic radii of the rare-earth ions (from Yb to La). This frequency range represents the vibrations of the oxygen octahedra, with RE/Ta in their interior. Changing the cations will affect the modes in the region 600–900 cm^{-1}, especially the A$_{1g}$ (O) peak (totally symmetric stretching of the TaO$_6$ octahedra). For this mode, the frequency decreased from 841 cm^{-1} for Yb to 808 cm^{-1} for ceramics with lanthanum. This result agree with the observations of Dias et al.,[22] who showed a clear correlation between the ionic radii of lanthanides and yttrium cations and the frequencies of the A$_{1g}$ mode, which decreased with increasing ionic radii (or unit cell volume).

4. Conclusions

Complex Ba(RE$_{1/2}$Ta$_{1/2}$)O$_3$ [RE = Y, Yb, Ho–Nd, and La] ceramics have been obtained by solid state ceramic route aiming applications as dielectric resonators. The materials presented high dielectric constants and quality factors and good thermal stability of the resonance frequency in the GHz range. The variations of the temperature coefficient of the resonance frequency with increasing RE atomic number was explained by lowering of symmetry, demonstrated by the peak splitting of Bragg reflections as well as the appearing of ferroelastic domains. Raman spectra allowed us to identify the symmetry groups of the samples: samples with Yb, Y and Ho are cubic and presented 4 intense Raman bands; ceramics with Dy, Tb, Gd and Eu are tetragonal, showing 9 bands; and, finally, materials with Sm, Nd and La are compatible with a orthorhombic group symmetry with 16 observed bands of the 24 predicted ones.

References

1. Wersing, W., *Electronic Ceramics*. Elsevier, London, UK, 1991.
2. Wersing, W., Microwave ceramics for resonators and filters. *Curr. Opin. Solid State Mater. Sci.*, 1996, **1**, 715–731.
3. Plourde, J. K., Linn, D. F., O'Bryan, H. M. and Thomson, J., Ba$_2$Ti$_9$O$_{20}$ as a microwave dielectric resonator. *J. Am. Ceram. Soc.*, 1975, **58**, 418–420.
4. Wolfram, G. and Gobel, H. E., Existence range, structural and dielectric properties of Zr$_x$Ti$_y$Sn$_z$O$_4$ ($x + y + z = 2$). *Mater. Res. Bull.*, 1981, **16**, 1455–1463.

5. Kamba, S., Petzelt, J., Buixaderas, E., Haubrich, D., Vanek, P., Kuzel, P. *et al.*, High-frequency dielectric properties of $A_5B_4O_{15}$ microwave ceramics. *J. Appl. Phys.*, 2001, **89**, 3900–3906.

6. Tamura, H., Konoike, T., Sakabe, Y. and Wakino, K., Improved high-Q dielectric resonator with complex perovskite structure. *J. Am. Ceram. Soc.*, 1984, **67**, C59–C61.

7. Sagala, D. A. and Koyasu, S., Infrared reflection of $Ba(Mg_{1/3}Ta_{2/3})O_3$ ceramics. *J. Am. Ceram. Soc.*, 1993, **76**, 2433–2436.

8. Hughes, H., Iddles, D. M. and Reaney, I. M., Niobate-based microwave dielectrics suitable for third generation mobile phone base stations. *Appl. Phys. Lett.*, 2001, **79**, 2952–2954.

9. Smolenskii, G. A., Isupov, V. A. and Agranovskaya, A. I., Dielectric polarization of solid solutions in the system $(Ba, Sr)_2(Ta, Nb)O_6$. *Soviet Phys. Solid State*, 1959, **1**, 909–911.

10. Galasso, F. S., *Structure, Properties and Preparation of Perovskite Type Compounds (1st ed.)*. Pergamon Press, Headington Hill Hall, Oxford, 1969, pp. 11–17.

11. Takata, M. and Kageyama, K., Microwave characteristics of $A(B_{1/2}^{3+}B_{1/2}^{5+})O_3$ ceramics. *J. Am. Ceram. Soc.*, 1989, **72**, 1955–1959.

12. Sreemoolanathan, H., Ratheesh, R., Sebastian, M. T. and Mohanan, P., $Ba(Tb_{1/2}Nb_{1/2})O_3$: a new ceramic microwave dielectric resonator. *Mater. Lett.*, 1997, **33**, 161–165.

13. Khalam, L. A., Sreemoolanathan, H., Ratheesh, R., Mohanan, P. and Sebastian, M. T., Preparation, characterization and microwave dielectric properties of $Ba(B_{1/2}'Nb_{1/2})O_3$ [B' = La, Pr, Nd, Sm, Eu, Gd, Tb, Dy, Ho, Y, Yb and In] ceramics. *Mater. Sci. Eng. B*, 2004, **107**, 264–270.

14. Korchagina, S. K. and Shevchuk, Y. A., Low-frequency and microwave dielectric properties of Ba_2LnTaO_6 [Ln = La, Pr, Sm, Dy, Ce, Gd, Nd, Tm, Tb] ceramics. *Inorg. Mater.*, 2006, **42**, 66–69.

15. Galasso, F. S., Layden, G. K. and Flinchbaugh, D. E., $Ba(B_{0.5}Ta_{0.5})O_3$ ordered perovskite-type compounds, possible new laser host materials. *J. Chem. Phys.*, 1966, **44**, 2703–2707.

16. Koshy, J., Kurian, J., Thomas, J. K., Yadava, Y. P. and Damodaran, A. D., Rare-earth barium niobates. *Jpn. J. Appl. Phys.*, 1994, **33**, 117–121.

17. Zurmühlen, R., Colla, E., Dube, D. C., Petzelt, J., Reaney, I. M., Bell, A. *et al.*, Structure of $Ba(Y_{1/2}^{3+}Ta_{1/2}^{5+})O_3$ and its dielectric properties in the range 10^2–10^{14} Hz, 20–600 K. *J. Appl. Phys.*, 1994, **76**, 5864–5873.

18. Zurmühlen, R., Petzelt, J., Kamba, S., Voitsekhovskii, C., Colla, E. and Setter, N., Dielectric spectroscopy of $Ba(B_{1/2}'B_{1/2}'')O_3$ ceramics: correlation between ionic parameters and microwave dielectric properties. *J. Appl. Phys.*, 1995, **77**, 5341–5350.

19. Gregora, I., Petzelt, J., Pokorny, J., Vorlicek, V., Zikmund, Z., Zurmühlen, R. *et al.*, Raman spectroscopy of the zone centre improper ferroelastic transition in ordered $Ba(Y_{1/2}Ta_{1/2})O_3$ complex perovskite ceramic. *Solid State Commun.*, 1995, **94**, 899–903.

20. Henmi, K., Hinatsu, Y. and Masaki, N. M., Crystal structures and magnetic properties of ordered perovskites Ba_2LnNbO_6 (Ln = Lanthanide elements). *J. Solid State Chem.*, 1999, **148**, 353–360.

21. Doi, Y. and Hinatsu, Y., Magnetic properties of ordered perovskites Ba_2LnTaO_6 (Ln = Y, lanthanides). *J. Phys.: Condens. Matter*, 2001, **13**, 4191–4202.

22. Dias, A., Khalam, L. A., Sebastian, M. T., Paschoal, C. W. A. and Moreira, R. L., Chemical substitution in $Ba(RE_{1/2}Nb_{1/2})O_3$ (RE = La, Nd, Sm, Gd, Tb, Y) microwave ceramics and its influence on the crystal structure and phonon modes. *Chem. Mater.*, 2006, **18**, 214–220.

23. Hakki, B. W. and Coleman, P. D., A dielectric resonator method of measuring inductive capacitance in the millimeter range. *IRE Trans. Microw. Theory Tech.*, 1960, **MTT-8**, 402–410.

24. Krupka, J., Derzakowski, K., Riddle, B. and Jarvis, J. B., A dielectric resonator for measurements of complex permittivity of low loss dielectric materials as function of temperature. *Meas. Sci. Technol.*, 1998, **9**, 1751–1756.

25. Hayes, W. and Loudon, R., *Scattering of Light by Crystals*. Wiley, New York, NY, 1978, p. 7, 31.

26. Reaney, I. M., Colla, E. and Setter, N., Dielectric and structural characteristics of Ba- and Sr-based complex perovskites as a function of tolerance factor. *Jpn. J. Appl. Phys.*, 1994, **33**, 3984–3990.

27. Rousseau, D. L., Bauman, R. P. and Porto, S. P. S., Normal mode determination in crystals. *J. Raman Spectrosc.*, 1981, **10**, 253–290.